Robotic Ankle–Foot Orthosis With a Variable Viscosity Link Using MR Fluid

Takahiro Oba, Hideki Kadone, Modar Hassan, *Member, IEEE*, and Kenji Suzuki, *Member, IEEE*

***Abstract*—This paper proposes a novel semiactive ankle–foot orthosis (AFO) called SmartAFO equipped with an elastic link mechanism. The design of the device is based on the understanding of gait biomechanics for gait assistance against paralysis and other gait abnormalities affecting the ankle joint function. The elastic link at the core of the developed AFO is a 1-degree-of-freedom linear-motion system, capable of regulating its viscosity via a magnetorheological fluid and an electromagnetic coil. The link is also integrated with a compression spring that allows it to store and release energy based on its coil current. This design enabled a semiactive AFO that can mitigate foot slap and toe drag without adversely affecting push-off or other gait phases. We present the development of SmartAFO and the results of experiments conducted on healthy people to verify its support functions compared to a commercial AFO. The results showed that SmartAFO can provide controllable braking torque at the heel contact, avoid ankle motion obstruction during the push-off phase, and support toe lift during the swing phase.**

***Index Terms*—Ankle–foot orthosis (AFO), ankle motion assistance, gait support, gait training, magnetomechanical effects, mechanical energy storage, MR fluid, semiactive mechanism, wearable device.**

I. Introduction

A. Background

THE ankle joint plays a critical role in gait function. The major functional tasks of gait, such as weight acceptance, single limb support, and limb advancement, depend on the proper functioning of the ankle joint. The ankle joint complex serves all these functional tasks, providing shock absorption and momentum control during weight acceptance, body weight support and balance control during single limb support, and propulsion and clearance from the ground during limb advancement [1].

Neurological and muscular pathologies, such as stroke, spinal cord injury, muscle atrophy, and cerebral palsy, affect the voluntary muscle control ability and muscle strength of the ankle joint complex; thus, severely impairing the gait function [1], [2].

Foot-drop is one of the common gait abnormalities [3], [4]. Foot-drop is characterized by the weakness or inability to control the dorsiflexor muscles, causing two major gait deficits: foot slap and toe drag. During weight acceptance (initial contact phase), the inability to control the deceleration of the foot causes the foot to "slap" on the ground instead of transitioning smoothly. This issue affects proper shock absorption, dynamic progression of gait, and body balance. During limb advancement (swing phase), the inability to dorsiflex the ankle joint results in insufficient clearance between the toes and the ground, causing abnormal compensative gait styles to maintain adequate clearance, or the toes being dragged on the ground if adequate clearance cannot be maintained. The foot slap and toe drag deficiencies severely affect gait function and are both causes of falling in people with foot-drop.

Among stroke patients in the acute phase, 70% fall in the first year and up to 47% fall in general. Among people with incomplete spinal cord injury, 75% fall at least once a year and 18% undergo a fracture because of a fall injury. Among postpolio patients, the numbers are 64% and 35%, respectively. Moreover, 65% of adults with peripheral neuropathy fall at least once during a year [5]. Although falls are multifactorial by nature, the biomechanical deficits of foot-drop are obvious contributors to the risk of falling. The most common treatment for such gait deficiencies is the use of an ankle–foot orthosis (AFO). An AFO is worn around the shank–ankle–foot complex to provide assistive forces, resist the unwanted motions and support the useful ones, and correct the foot posture.

The purpose of this paper is to develop the mechanism and prototype of a semiactive AFO for the ambulatory support of people with gait deficiencies. The target support functions are dynamic braking during weight acceptance to mitigate foot slap and assisted dorsiflexion during swing phase to mitigate toe drag. Another design objective is to avoid ankle motion obstruction during the push-off phase, i.e., not to hinder forward propulsion with the AFO prior to weight acceptance on the contralateral side leg (see Table I). This paper introduces the

Manuscript received February 7, 2018; revised April 27, 2018 and August 17, 2018; accepted December 31, 2018. Date of publication January 21, 2019; date of current version April 16, 2019. Recommended by Technical Editor H. A. Varol. This work was supported in part by the Funding Program for World-Leading Innovative R&D on Science and Technology (FIRST Program),World leading human-assistive technology supporting a long-lived and healthy society, and in part by the Japan Society for the Promotion of Science KAKENHI under Grant 17H01251. *(Corresponding author: Modar Suleiman Hassan.)*

T. Ohba is with the Graduate School of Engineering System, University of Tsukuba, Tsukuba 305-8577, Japan (e-mail: taka@ai.iit.tsukuba.ac.jp).

H. Kadone is with the Center for Innovative Medicine and Engineering, Center for Cybernics Research, University of Tsukuba Hospital, Tsukuba 305-8576, Japan (e-mail: kadone@ccr.tsukuba.ac.jp).

M. Hassan is with the Faculty of Systems and Information Engineering, University of Tsukuba, Tsukuba 305-8573, Japan (e-mail: modar@ai.iit.tsukuba.ac.jp).

K. Suzuki is with the Faculty of Engineering, Center for Cybernetics Research, University of Tsukuba, Tsukuba 305-857, Japan (e-mail: kenji@ieee.org).

Digital Object Identifier 10.1109/TMECH.2019.2894406

TABLE I
COMPARISON OF THE FUNCTIONS OF A POSTERIOR PLASTIC AFO, GAITSOLUTION, AND SMARTAFO

	Initial contact phase	Push-off phase	Swing phase
Posterior plastic AFO	Fixed plantarflexion	Fixed plantarflexion	Prevent plantarflexion
GaitSolution	Braking plantarflexion (manually adjustable force)	Braking plantarflexion	Assist dorsiflexion
SmartAFO	Braking plantarflexion (adjustable force)	Free plantarflexion	Assist dorsiflexion

prototype of the developed AFO, its mechanical design, characterization, and evaluation with healthy people.

B. Related Work

Active and semiactive AFOs have received adequate attention but only a few solutions have made their way to practical implementation as daily support products. AFO technology can be broadly divided into passive, semiactive, and active technologies. Common designs of passive AFOs include nonarticulate thermoplastic types, such as a posterior plastic AFO, and articulate metal AFOs constructed from lateral metal uprights, hinges, foot holder, and straps [6], [7]. These AFOs limit the foot posture and motion; thus, preventing detrimental conditions such as excessive foot rotation and toe drag. As maintaining adequate toe clearance during the swing phase dramatically improves the gait function and owing to their low weight, reliability, robustness, and economic viability, passive AFOs remain most widely used.

The nonarticulate AFOs encompass portions of the leg ankle–foot complex, thus constraining its movement. The material properties and geometry of the AFO govern its mechanical deformation properties and, thus, the amount of motion resistance (stiffness) it exerts on the ankle joint [8]. However, because of the fixed construction of such AFOs, they resist useful motions such as foot plantarflexion during the push-off phase. Restricting the ankle joint motion might compromise important balance and postural control mechanisms during gait [9].

This has led to the development of more sophisticated types of passive AFOs with additional passive motion control elements. These are referred to by some researchers as "hybrid" AFOs [10]. The passive motion control elements used are hydraulic (or pneumatic) dampers or springs [11]. The most relevant example to our study is the GaitSolution AFO developed over several years by Yamamoto *et al.* at the International University of Health & Welfare, Japan [12] (see Table I). GaitSolution implements a novel solution to prevent foot slap and toe drag by utilizing an oil damper and a compression spring acting on the ankle joint in an articulate-structure AFO. The AFO has two joints in the lateral and medial sides. The oil damper and the spring act on the lateral side joint in the plantarflexion direction. In earlier studies, Yamamoto *et al.* [11], [13] revealed some of the desired characteristics of AFOs. They focused on characteristics needed for hemiplegic patients and conducted experiments using a custom-made experimental AFO with exchangeable dorsiflexion and plantarflexion assist springs. Their findings showed that some of the important characteristics paramount to AFOs include the possibility of adjusting the initial ankle angle and the resistive moment against plantarflexion (5 to 20 N·m of plantarflexion-resist moment per 10° of plantarflexion). They also argued that an AFO should not generate resistive moment against dorsiflexion. In the second part of their investigation, they developed an AFO with such characteristics, namely dorsiflexion assist controlled by spring AFO, using an oil damper with a spring installed posterior to the ankle joint. They compared the developed AFO with a posterior leaf AFO for five hemiplegic patients and demonstrated an improvement in the walking velocity for all the participants. The design was then modified into the current version of the AFO, named "GaitSolution," with the oil damper installed laterally to the ankle joint (2 to 20 N·m of plantarflexion-resist moment per 10° of plantarflexion) [14].

Active AFOs, on the other hand, use powered actuators to directly assist the ankle joint. Therefore, they have much more potential in terms of the assisting function they can offer, particularly the ability to provide plantarflexion assistance in the push-off phase to propel the body forward. Examples of such active AFOs include the MIT Active AFO [15] and the Arizona State Robotic Tendon AFO [16], both of which utilize a series elastic actuator (SEA) consisting of a dc motor with a ball screw mechanism in series with a compression spring. Using the SEA, these systems can adjust the impedance around the ankle joint in different gait phases to realize the assist function. The AFOs have shown promising results in healthy and locomotion impaired people; however, they require further modification to serve as wearable and portable solutions for daily support. Moreover, although these systems use powered actuators, they have not been used for push-off assistance and were only shown to prevent foot slap and toe drag. To the best of our knowledge, there are currently no practical and untethered (battery-powered) active AFOs available as a commercial product for daily support [10].

C. Concept

Yamamoto *et al.* investigated the role of adjustability as an essential characteristic for future AFOs [13]. Appropriate setting of the initial angle and braking moment in loading response do not only mitigate foot slap, but also affect the alignment of the thigh and shank during stance and the magnitude and direction of the ground reaction force vector.

However, there are inherent limitations with the use of only passive technology in terms of adjustability. Passive elements, such as springs and valves, function in an open-loop manner; thus, limiting their adaptability to changing walking conditions or functional tasks. Moreover, passive devices hinder useful portions of the gait cycle, such as the push-off phase. Therefore, the switch to semiactive technology could improve the AFO robustness and adjustability via a sensor-based closed-loop control.

Based on the above brief review of the AFO technology, we conclude that a semiactive technology is more appropriate for the mitigation of foot slap and toe drag and for the correction of foot posture. In particular, the use of magnetorheological (MR) fluid dampers has the potential to selectively modulate the

impedance around the ankle joint in coordination with the force and/or angle in a closed-loop manner. Kikuchi *et al.* [17] developed an AFO with a disk-type rotary MR brake to mitigate foot slap and toe drag. Svensson *et al.* [18] developed an AFO with a linear MR damper and proposed control algorithms for the AFO under level walking, inclination walking, and stair climbing and descending. These works along with the investigations on GaitSolution motivated this study to investigate and develop a new semiactive AFO with the MR technology. In the studies conducted by Kikuchi *et al.* [17] and Svensson *et al.* [18], MR dampers were used without a spring to enable energy storage and release function and without a mechanism to disengage the damper from the ankle joint to allow free ankle joint extension in the push-off phase. In this paper, we develop an AFO with an MR damper including these functions and demonstrate their mechanical effects on the ankle joint with healthy participants.

The aforementioned studies demonstrate the potential of MR fluid in orthopedic devices. Alternative functional fluids, such as electrorheological fluid, can help realize faster response time. However, an MR fluid exhibits higher material performance (field-dependent yield stress), making it more viable to realize a compact wearable device. Variable damping and clutch functions can also be achieved with a hydraulic piston and servo valves, as in the case of some computer-controlled prosthetic knees [19]. However, using servo valves considerably increase the size and complexity of the system and drastically increases the total cost. Moreover, the viscosity of oil changes with temperature, making oil-based devices less reliable in hot or cold weather.

Here, we propose a semiactive AFO, called SmartAFO, that can mitigate foot slap and toe drag without adversely affecting the push-off or other gait phases. SmartAFO uses an elastic link mechanism, called MRLink, wherein an MR fluid is used along with a compression spring. MR fluids have been implemented in the AFO technology with successful results [18], [20]. MRLink utilizes the characteristics of embedded MR fluid and compression spring to regulate its damping and the interaction force with the ankle joint during gait and thereby provide physical assistance to the wearer.

II. Link System With Variable Viscosity: MRLink

A. Basic Structure and Motion Principle

MRLink is a 1 degree-of-freedom linear-motion system, consisting of an interaction rod, a cylinder, a piston with an electrical coil, a spring, and MR fluid (see Fig. 1). While the rod is nonmagnetic, the cylinder and piston are made from magnetic materials. When the coil is excited, a magnetic field is generated, and the MR fluid in the gap between the cylinder and the piston is magnetized [see Fig. 1(c)], yielding a proportionate shear force between the piston and the cylinder. The generated force depends on the magnetic field strength and works against the interaction force and the restoring force from the embedded spring. This shear force is a function of the shear velocity. Therefore, it can be considered variable viscosity. Table II lists the physical properties of MRLink.

A key factor is the combination of the MR fluid effect and the compression spring inside MRLink. This combination presents

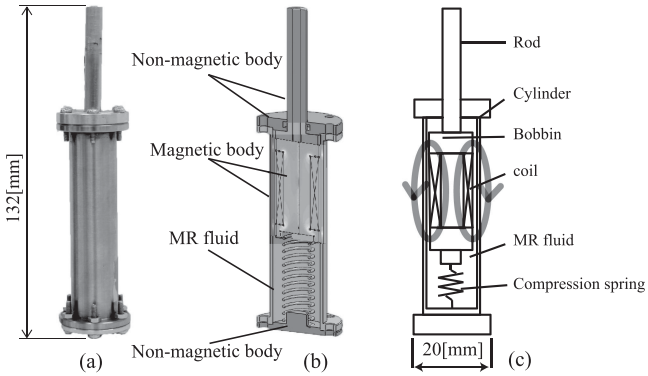

Fig. 1. (a) Appearance and (b) internal structure of MRLink. The cylinder and the bobbin are made from a magnetic material with high permeability. The interaction rod and the top and bottom caps are made from nonmagnetic materials. A compression spring is embedded between the bobbin and the bottom cap. The internal space is filled with an MR fluid, and the gap between the bobbin and the cylinder represents the active volume where the magnetic field passes through the MR fluid. (c) Schematic representation of MRLink. The loops with directional arrows represent the flow of the magnetic field through the bobbin, the gap with MR fluid, and the body of the cylinder.

TABLE II
Physical Characteristics of MRLink

Total weight	162 g
Spring constant	0.75 N/mm
Number of turns	450 turn
Magnetic gap	1.0 mm
Use of MR fluid	8.6 cm^3
Maximum stroke	30 mm

a unique property from a force management viewpoint; MRLink can retain the force acting on the internal spring via the yield stress of the MR effect, and the retained force can be released later by turning off the excitation of the MR fluid. Using this force retention mechanism, MRLink can manage the interaction force with physical systems and can achieve several tasks without the need for an external actuator. This property is utilized to achieve toe clearance in SmartAFO, as shown later in Section III-C.

B. Modeling

The braking force developed by an MR fluid device depends on the operation mode, construction, and morphology of the device and the strength of the magnetic field. MR fluid devices have mainly two modes of operation: shear mode and valve mode [21]. MRLink operates in the shear mode, implying that it utilizes the shear forces developed between a fixed surface and a moving surface with MR fluid in between. The developed braking force can be calculated using the following equation:

$$F = F_r + F_{mr} = \frac{[\eta S A]}{g} + \tau A \tag{1}$$

where F is the total developed braking force, F_r is the component of the force due to the rheology and flow of the fluid inside the device, F_{mr} is the component of the force due to the magnetic field, η is the MR fluid viscosity, S is the relative fluid-pole velocity, A is the shear area, g is the gap between

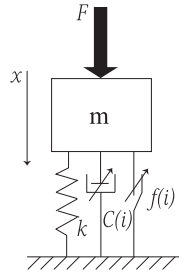

m	Mass
k	Spring constant
F	External force
C(i)	Total viscosity
f(i)	Yield strength
i	Coil current

Fig. 2. Modeling and model parameters of MRLink.

the poles, and τ is the yield stress developed in response to the applied magnetic field.

The dynamic behavior of MRLink in a system is, however, more complicated. The force in a dynamic scenario can be divided into inertia (mass), viscosity (damping), and stiffness components. Thus, we propose a dynamic model for MRLink including the elements that are regulated by the current in the coil (see Fig. 2) [22] as follows:

$$\text{if} \quad |F - kx| \leq |f(i)|$$
$$\text{then} \quad x = \text{constant} \tag{2}$$
$$\text{else} \quad m\frac{d^2x}{dt^2} + C(i)\frac{dx}{dt} + kx = F \tag{3}$$

where $f(i)$ represents the yield strength of the MR fluid, which is a directional force that depends on the coil current. $f(i)$ increases monotonically with respect to i. k is the spring constant of the compression spring embedded inside MRLink, F is the external load force acting on the interaction rod, x is the linear position displacement of the tip of the interaction rod, i is the coil current of MRLink, m is the mass of the system, and $C(i)$ is the total viscosity of the system.

When the total force acting on the interaction rod is lower than the yield strength, the system stays static and behaves according to (2). It is important to note that $f(i)$ is a resistive force and, thus, changes direction to assist or to counteract the spring against the external force. When the external force or the spring-generated force is greater than the yield strength, the system behaves as a spring-damper system according to (3).

The components $f(i)$ and $C(i)$ can be controlled by the applied magnetic field, which in turn is controlled by the current in the coil. Therefore, MRLink affects both the viscosity and the offset of the holding force of the system. Such a behavior of MRLink requires verification with empirical experiments.

III. Ankle–Foot Orthosis: SmartAFO

A. Development of SmartAFO

Here we describe in detail the developed SmartAFO, which is an ankle–foot orthosis based on MRLink (see Fig. 3). The original AFO was developed by Kowagishi Laboratory Co., Ltd. It has two metal bars with an articulated ankle joint, resulting in one free degree-of-freedom for dorsiflexion and plantarflexion.

We equipped the AFO with MRLink, a control circuit, a battery, and sensors. The entire system weighs 819 g while the weight of the original AFO is 493 g. Table III lists the physical

Fig. 3. Overview of SmartAFO. The base frame is an articulated AFO with two metal bars. MRLink is fixed to the lateral bar. A 3-D printed cover is also fixed to the lateral bar, with battery and control circuit embedded inside. A simple mechanism is used to convert the linear force of MRLink into a rotary moment about the ankle joint.

TABLE III
Physical Characteristics of SmartAFO

Height	380 mm
Length	260 mm
Width	95 mm
Weight(original AFO)	493 g
Total weight	819 g
Maximum power consumption	5 W
Maximum braking torque	1.88 Nm

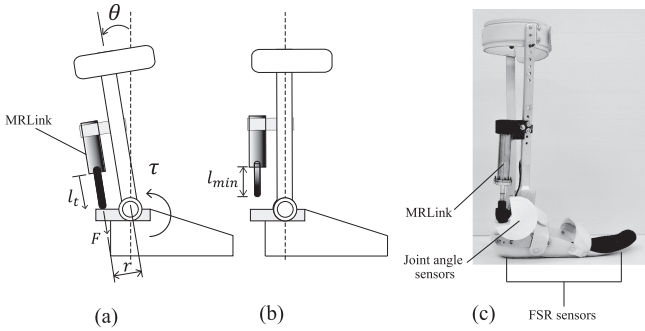

Fig. 4. Schematic of SmartAFO. MRLink is installed on the back side of the AFO. A simple mechanism converts the force of MRLink into a torque about the ankle joint. (a) MRLink acting on the ankle joint with a plantarflexion braking torque. (b) MRLink while contracted (maximum coil current after the spring compression); thus, maintaining a free gap between its interaction rod and the foot segment. (c) The real device.

characteristics of SmartAFO. We designed a simple mechanism to convert the linear motion of MRLink into a rotary motion around the ankle joint and housed the mechanism with a 3-D printed cover. The battery and the control circuit are fitted inside the housing as well. Fig. 4 shows the function of the designed mechanism. From this mechanism, the moment arm whereby the MRLink acts on the ankle joint is denoted by r

$$\tau = rF. \tag{4}$$

The braking torque is defined by the applied coil current and the displacement of the compression spring. We empirically measured the braking forces generated by MRLink with the

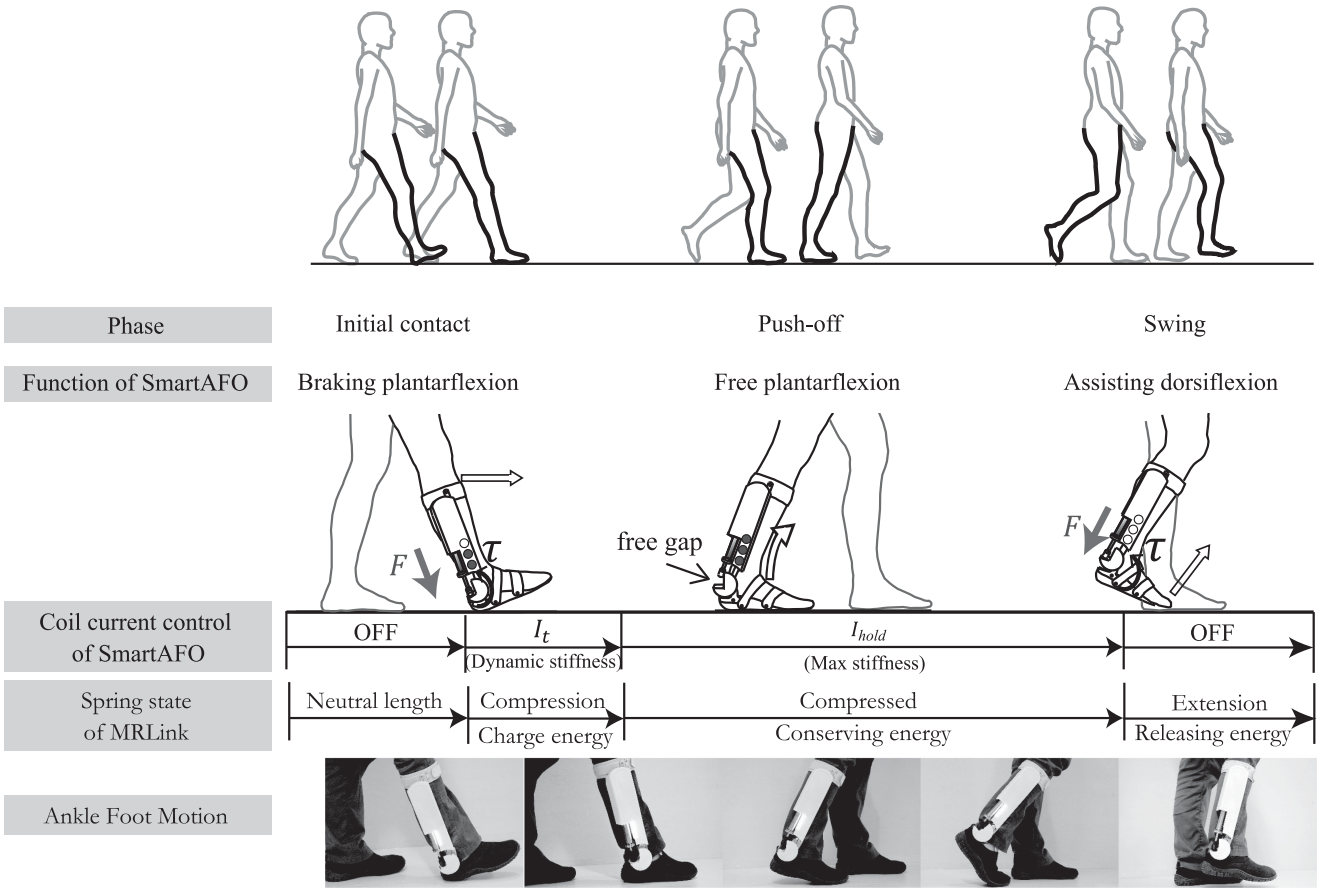

Fig. 5. Ankle motion assistance with SmartAFO. *Initial contact:* SmartAFO brakes the plantarflexion to smoothly assist initial contact. *Preswing:* SmartAFO holds the spring compressed during mid-stance and push-off to keep a free gap between the braking element and the foot segment so that a free plantarflexion is secured. *Swing:* SmartAFO releases the spring to assist dorsiflexion and prevent toe drag.

active MR fluid when fully extended and when its compression level is 20° of plantarflexion. We then calculated the braking torque acting on the ankle joint with a 5-cm moment arm. The braking torques were found to be 1.05 and 1.88 N·m when the ankle joint is in the neutral position (0°) and when it is plantarflexed (20°), respectively.

As shown in Fig. 4, MRLink is installed on the back side of the AFO. Thus, the braking torque generated by MRLink acts on the plantarflexion. The dorsiflexion is then assisted by releasing the force held in the spring during the previous braking phase.

B. Gait Phase Detection

The control method of smartAFO (see Fig. 5) requires realtime gait phase detection to set the coil current of MRLink. For this purpose, we implemented gait phase detection using the insole foot pressure and ankle angle. We installed a force sensor in the shoe insole under the heel and devised an ankle angle sensor using a potentiometer. The microprocessor on the control circuit inside the housing uses the sensor data to estimate the current gait phase and control MRLink accordingly. The gait phases are estimated from the salient characteristics of the ankle joint angle and angular velocity and the heel ground contact data. Fig. 6 shows an actual clip of the measured data. The circles indicate the start points of each phase detected from the preconfigured thresholds.

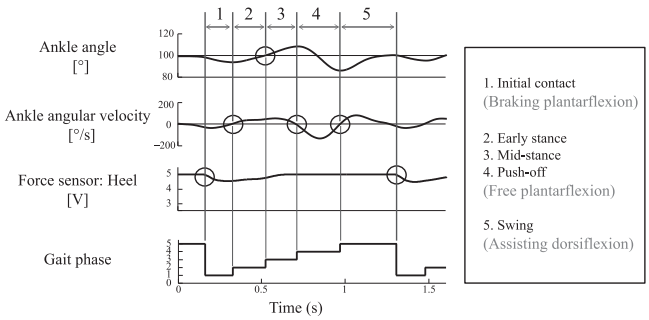

Fig. 6. Gait phase estimation based on sensor values of ankle angle, angular velocity, FSR toe, and FSR heel. The plot shows the sensor signals for three consequent gait cycles with the identified gait phases. The circular markings on the signals indicate the key events used for gait phase identification.

C. Gait-Phase-Based Ankle Assist

SmartAFO aids the ankle joint depending on the detected gait phase. This function is illustrated in Fig. 5.

The functional operation of SmartAFO can be divided into three stages corresponding to, first, the initial contact phase, second, the push-off phase, and last, the swing phase.

1) Initial Contact Phase: When the initial contact is detected, the braking torque is applied to prevent foot slap. The braking torque can be adjusted for individual users by

adjusting the coil current and is defined experimentally at this stage.

2) Push-off Phase: At the end of the initial contact phase, MRLink is compressed, and the current in the coil is increased to maximum. Consequently, MRLink is held in this condition, preserving the force inside the spring and maintaining a free gap between the interaction rod and the rotational mechanism of the ankle. With this method, SmartAFO does not obstruct plantarflexion at this stage.
3) Swing Phase: At this stage, after the foot departs from the ground, the current of MRLink is turned OFF, thereby releasing the preserved force in the spring and pushing the foot up to achieve toe clearance.

IV. Experiments

We devised a set of experiments to characterize the performance of MRLink and to verify the function of SmartAFO. The experiments with human participants were approved by the Internal Review Board of University of Tsukuba Hospital (H27-096).

A. Experiment 1: Characterization of MRLink Performance

1) Objective and method: The interaction force between MRLink and the external load is regulated based on the spring embedded inside MRLink and its coil current. To specify these characteristics, we devised an experimental workbench to test the variation in the damping of MRLink with respect to different springs and coil currents.

The workbench, shown in Fig. 7, consists of MRLink fixed using 3D-printed support beams, a laser sensor to measure the displacement of the interaction rod, and load cells to measure the force between the interaction rod and the external load. A robot manipulator (UR5, Universal Robots) is used to apply a sinusoidal load on the MRLink; the force is always greater than the yield strength of MRLink. MRLink was tested using four embedded springs with spring constants of 0.5, 0.75, 1.32, and 1.64 N/mm and for five coil currents of 0, 0.25, 0.5, 0.75, and 1 A. For each condition, the robot was operated to change the sinusoidal load frequency between 0.2 and 5 Hz with ten increments and then ten decrements. MRLink was actuated by the robot for ten full strokes at each frequency step, and five measurements were acquired for each condition. The load cell and laser sensor were connected to a DSP system (sBOX II. MTT Corp.) to collect synchronized data during the experiment at 1 kHz. The acquired sensor data were then processed using MATLAB code to estimate the viscosity of MRLink.

2) Result: Fig. 8 shows the outcome of this test. The viscosity was regulated approximately between 100 and 400 Ns/m with a good linear correlation with the increasing coil current. However, the viscosity–current characteristics with the 1.32 N/mm spring are less linear than with other springs.

We tested the holding force of MRLink; the holding force is the force required to displace the interaction rod under a static condition with incremental coil currents (0–1 A with 0.2 increments). An incremental force was applied to MRLink when fully extended, and the force value at which the rod of MRLink starts to sink into the cylinder was recorded. The results show that MRLink can develop up to 30 N of holding force (see Fig. 9).

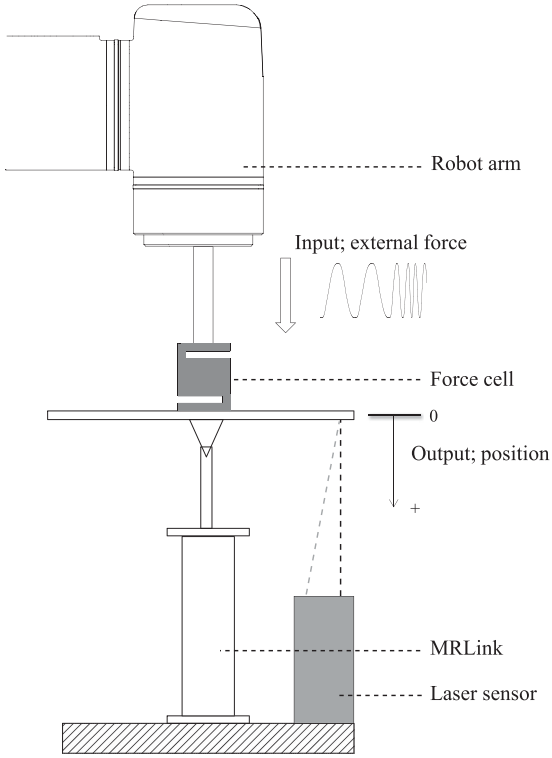

Fig. 7. Overview of the workbench used to evaluate the mechanical impedance characteristics of MRLink. A robot arm is used to apply loads on MRLink. A load cell is used to measure the force applied on the interaction rod of MRLink, and a laser sensor is used to measure its displacement.

In addition, we tested the battery life of MRLink during walking assistance. For this purpose, we prepared a test environment and continuously controlled the coil current to simulate walking assist; the coil current was set to 0.5 A during initial contact, 1 A during midstance and preswing, and 0 A during the swing phase. The system was started with a fully charged battery (7.4 V; 1000 mAh) and was run until the battery was drained. The gait step counter was streamed to a logging computer via Bluetooth. The result shows that over 4000 steps can be achieved per full battery charge.

3) Discussion: The results of the holding force developed by MRLink show early saturation starting from a coil current of 0.2 A (see Fig. 9). This is probably because of the early saturation of the magnetic field developed in the bobbin or carried in the cylinder. In addition, the limited maximum force of 30 N makes the applicable range of SmartAFO rather limited when compared to the wide range of joint stiffness provided by other AFOs [13].

This result shows that the total viscosity of MRLink $C(i)$ can be considered to consist of the innate viscosity of the MR fluid c and the shear force developed by the MR effect $c_f(i)$, as in (5)

$$C(i) = c + c_f(i). \tag{5}$$

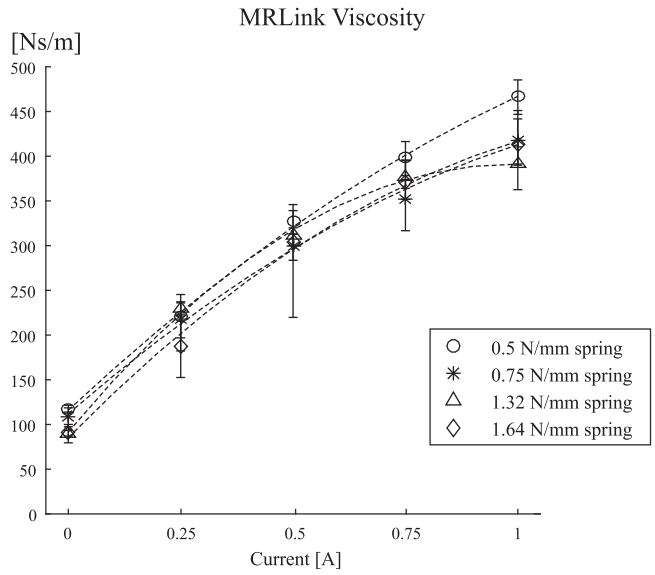

Fig. 8. Empirical evaluation of the viscosity of MRLink with different springs and incremental coil currents. The graphs show mean values with error bars, and the dotted lines indicate the second-order polynomial fits of the mean values.

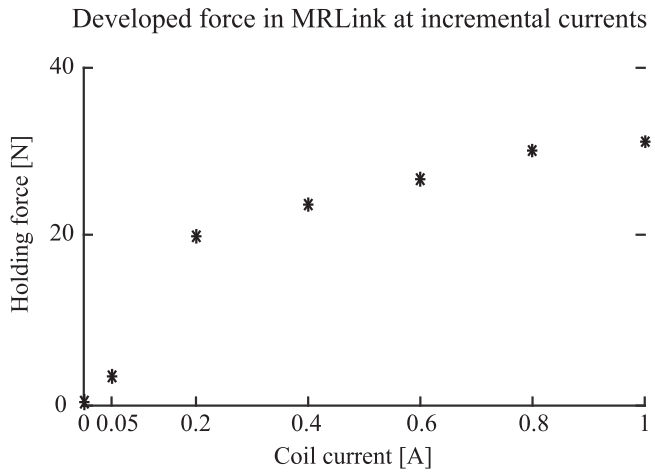

Fig. 9. Empirical evaluation of the static holding force developed by MRLink.

B. Experiment 2: Assisting Ankle Motion by SmartAFO

1) Objective and Methods: This experiment was conducted to verify the feasibility of assisting ankle motion in real time by SmartAFO during walking in healthy persons and compare its function to an alternative AFO with similar functionality, namely the GaitSolution. GaitSolution is similar to SmartAFO in that it uses a linear motion damper with a compression spring installed on the lateral bar of the AFO and in the assist function it provides during the initial contact phase. However, GaitSolution uses only passive components to achieve its function; an oil damper and a compression spring, making its mechanism very robust and compact. GaitSolution and SmartAFO provide different assist functions during the swing phase, wherein GaitSolution only resists plantarflexion, whereas SmartAFO assists active dorsiflexion using the force stored in the spring during the earlier initial contact phase. SmartAFO uses sensors to control the assist function in a semiactive manner, whereas GaitSolution allows mechanical adjustment of the initial angle and resistive force before wearing the AFO. GaitSolution and SmartAFO weigh 380 and 819 g, respectively.

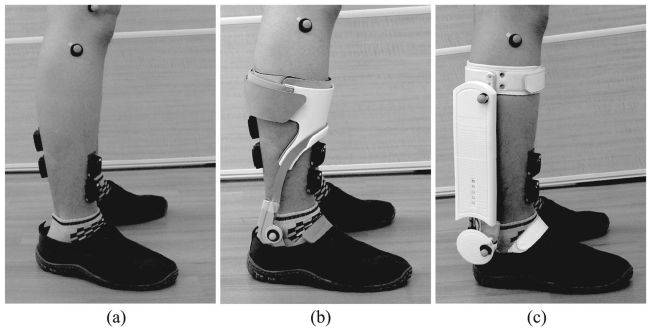

Fig. 10. Conditions of walking in the experiments to evaluate ankle motion assist by SmartAFO: (a) without AFO, (b) with GaitSolution (GS), and (c) with SmartAFO.

In this experiment, seven healthy participants walked on a straight 10 m path twice under each of the following conditions (see Fig. 10).

1) Without AFO.
2) With GaitSolution (GS).
3) With SmartAFO/Coil current: 0.0 A.
4) With SmartAFO/Coil current: 0.5 A.
5) With SmartAFO/Coil current: 1.0 A.

In the conditions that included the AFO, the participants wore the AFO on the right foot and a shoe of the same size on the left foot. The spring constant of the spring used in the experiments was 1 N/mm. The coil current of MRLink was controlled in the manner described in Section IV C; either 0.0, 0.5, or 1.0 A during the initial contact phase, 1.0 A during the preswing phase, and 0.0 A during the swing phase (see Fig. 5).

We measured the activity of the dorsiflexor muscles and plantar flexor muscles using a wireless EMG system (Trigno, Delsys Inc., USA) and the 3-D kinematics of the lower limbs using a motion capture system (VICON MX with 16 T40 cameras, U.K.). The participants walked at a cadence of 90 step/min according to a metronome.

2) Results and Discussions: For the analysis, 18 steps were extracted under each walking condition for each participant. For each step, the integrated EMGs of the dorsiflexor muscles, plantar flexor muscles, ankle angle, and ankle angular velocity were calculated. These values were then processed for each gait phase as follows. This calculation was done for each participant and then averaged for all participants. Fig. 11 shows the three evaluation indices. The results were normalized with respect to the value corresponding to normally walking without the AFO.

Initial Contact Phase: In the initial contact phase, the required function of the AFO is to brake the plantarflexion. Therefore, we calculated the average ankle joint angular velocity over the initial contact phase obtained under the different experimental conditions [see Fig. 11(a)]. The index values are, in comparison to walking without AFO, 0.62 times with GS, 0.89 times

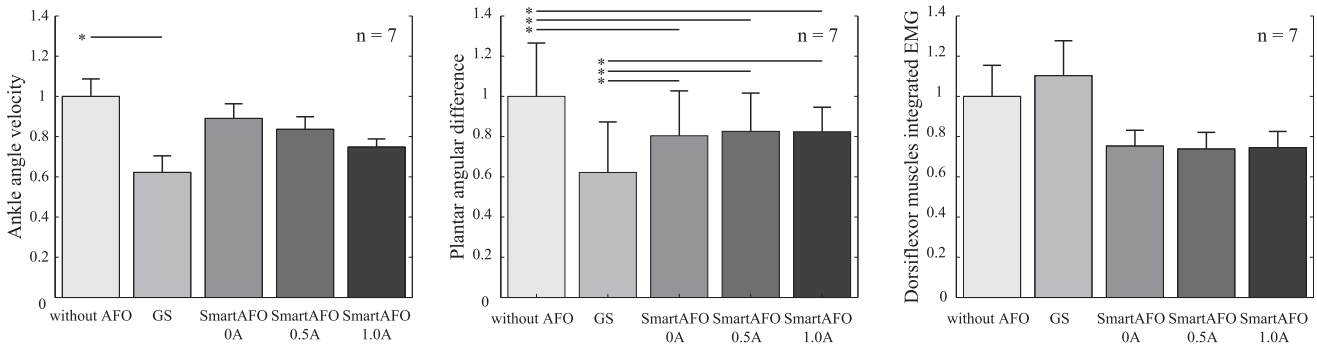

Fig. 11. Results of the ankle motion assist experiment. The plots show the average and standard deviation values for: walking without AFO, walking with GaitSolution (GS), walking with SmartAFO at 0 A, walking with SmartAFO at 0.5 A, and walking with SmartAFO at 1 A. The values in each bar plot are normalized with respect to the value obtained under "without AFO" condition. (a) Average ankle angular velocity during the initial contact phase. (b) Ankle plantar angular difference during the preswing phase. (c) Integrated EMG value of the ankle dorsiflexor muscle during the swing phase.

with SmartAFO at 0.0 A, 0.83 times with SmartAFO at 0.5 A, and 0.74 times with SmartAFO at 1.0 A. The ankle angular velocity when walking without AFO before normalizing is 92.4°/s. Only the difference between without AFO and GS conditions was statistically significant.

The results showed that GS introduced the lowest velocity (highest braking effect) during initial contact. Moreover, the results showed a systematic relationship between the coil current and the angular velocity with SmartAFO. This is consistent with the design, with greater coil current, the viscosity increases which leads to a higher braking torque and hence to lower angular velocity. This demonstrates the controllability of the braking force via the coil current, which can be used to customize support for each individual user depending on his/her muscle strength and functional condition.

Push-off Phase: In the push-off phase, the proposed action by SmartAFO and GaitSolution is to secure a free plantarflexion without obstructing the ankle joint. Therefore, we compared the displacement of the ankle angle from heel lifting to toe lifting [see Fig. 11(b)]. A larger displacement of the ankle angle implies that the ankle joint is sufficiently plantarflexed during this phase. The index values were, in comparison to walking without AFO, 0.62 times with GS, 0.80 times with SmartAFO at 0.0 A, 0.82 times with SmartAFO at 0.5 A, and 0.82 times with SmartAFO at 1.0 A. The displacement of the ankle angle without the AFO before normalizing was 30.2°. Difference between the without AFO condition and each of the SmartAFO conditions was statistically significant. Difference between the GS and each of the SmartAFO conditions was statistically significant.

This index represents the amount of hindrance the AFO might be inflicting on the user during push-off. The displacement of the ankle angle was the smallest under the GS condition, implying that it adversely affects the ankle function in this phase. We consider that this effect is due to the uncontrollability of the braking mechanism in GaitSolution; the stiffness can only be adjusted before wearing the AFO. The plantarflexion of the ankle joint in this phase is somewhat near the range of that during initial contact. This engages the coil spring in the push-off phase, causing such a negative effect. SmartAFO can maintain a free gap between the braking mechanism and the foot segment during stance and thereby avoids this issue. In the case of SmartAFO, the value was lower than that under the no AFO condition but greater than that under the GS condition. Moreover, the value was independent of the control condition, as the control current was adjusted only during the initial contact phase (the control current under all the SmartAFO conditions in this phase is 1 A to halt the compression spring of MRLink). As MRLink in this phase is halted with the spring fully compressed, a free gap is created between the interaction rod and the foot segment, implying that the hindrance introduced is due to the construction of the base AFO brace and not due to the mechanism installed on top of it. We speculate that improvements to the basic construction of the AFO body and articulation could help alleviate this issue.

To confirm that a free gap is maintained between the interaction rod of MRLink and the foot segment, we measured the gap during gait using optical markers. The result (see Fig. 12) confirms that a free gap is maintained during the push-off phase, and the average gap size is greater than 10 mm at the moment of foot departure from the ground.

Swing Phase: In the swing phase, the required function of the AFO is to assist the dorsiflexion of the ankle joint to prevent toe drag. Therefore, we compared the integrated EMG of the dorsiflexor muscles to evaluate the effort they exert in maintaining the toe clearance under each condition [see Fig. 11(c)]. The index values were, in comparison to walking without AFO, 1.10 times with GS, 0.75 times with SmartAFO at 0.0 A, 0.73 times with SmartAFO at 0.5 A, and 0.74 times with SmartAFO at 1.0 A. The differences between conditions were not statistically significant for this index.

With regard to the EMG-related index, a high activation implies that the user must apply more muscle power to achieve the toe clearance during swing. A lower activation implies higher support for toe clearance from the AFO; thus, requiring less muscle power from the user. Here, we recorded a higher muscle activation when using the GS, whereas a lower muscle

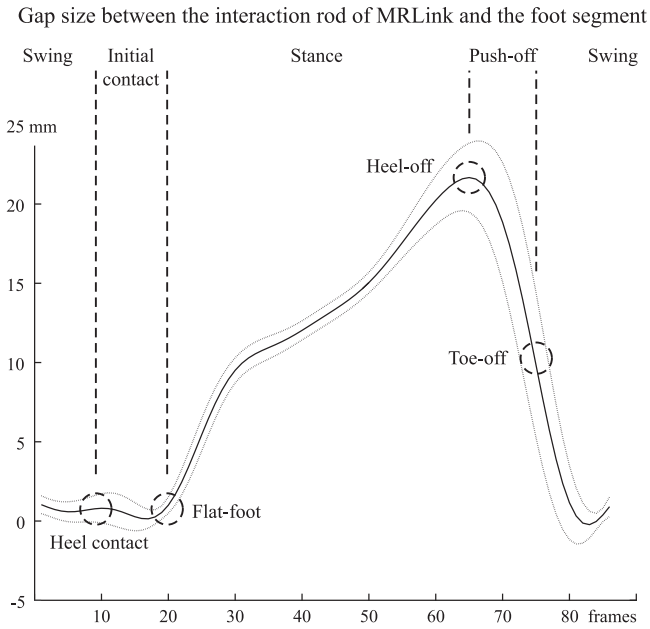

Fig. 12. Gap size between the tip of MRLink and the actuation arm of SmartAFO. The data are averaged for five strides of a healthy person walking with SmartAFO. The solid line indicates the mean value, and the dotted lines indicate the standard deviation.

activation was recorded when using SmartAFO compared to walking without an AFO. We speculate that in the case of GS, the plantarflexion in the push-off phase was insufficient, resulting in a poor propulsion of the foot and therefore requiring more muscle activity in this phase compared to that under the normal walking condition. When using SmartAFO under the different conditions, the dorsiflexor muscle activation was found to be at a similar level, implying a consistent assist action, achieved by releasing the spring force. The muscle activation was lower than that in the case of no AFO, indicating that such an assistance can be helpful for maintaining toe clearance.

V. Discussions

The first experiment serve to characterize the performance of MRLink when evaluated in two unique operation modes: when it is static as it exhibits a holding force and when it is in motion as it exhibits viscous resistance to motion, i.e., damping. The holding force of MRLink depends on the shear force exerted by the MR fluid on the friction surface and was shown to monotonically increase with the increase in the coil current with the spring fully extended, i.e., excluding the spring effect. Previous investigations showed that the required braking torque at initial contact ranges between 5 to 20 N·m per 10° of plantarflexion [13]. Reference textbooks on biomechanics [23] list the typical ankle joint moment in the sagittal plane at initial contact to be approximately 0.15 N·m per kg of body weight. For a person weighing 60 kg, this would result in a joint moment of 9 N·m. The developed MRLink has a maximum holding force of 30 N, a 1 N/mm spring, and only 5 cm moment arm when installed in SmartAFO. A simple calculation shows that it provides 1 N·m at the neutral position and 1.88 N·m at 20 of plantarflexion. Thus, its output is insufficient for a wide range of AFO users. Improving the power output of MRLink is necessary for the practical implementation in the AFO technology.

Several factors can be considered to improve the MRLink in the future. From (1), we note that the gap size between the bobbin and the cylinder can be decreased, and the friction surface area of the MR fluid can be increased to obtain a higher force output. The magnetic circuit design, bobbin, and cylinder shape, and material can be improved to avoid the saturation and strengthen the magnetic field on the friction surface. Materials with higher magnetic permeability can be used for the magnetic components. A good design of MRLink will require a balance between the mechanical, rheological, and magnetic properties. With the proposed improvements, we expect to increase the power output of MRLink to meet the requirements of AFO gait support.

The human experiment was designed to characterize the function of SmartAFO against GaitSolution in key aspects of the gait cycle with healthy participants. Regardless of the amplitude of the support action, the conducted experiments with healthy persons helps us to verify the developed AFO's benefits from several aspects. The ankle angular velocity during initial contact demonstrated the braking effect of MRLink, which is proportional to the coil current. The plantar angular difference of the ankle joint from heel lifting to toe lifting showed less hindrance when using SmartAFO compared to GaitSolution, and the dorsiflexor muscle EMG showed less activation during swing compared to walking without AFO and compared to walking with GaitSolution. This shows that maintaining a free gap between the braking element and the foot segment during push-off could reduce hindrance and alleviate subsequent effects on following gait phases. The experiments were conducted only on healthy participants and cannot be extrapolated to people with gait disabilities. The experiments serve to investigate the mechanistic effect of the developed device on the ankle joint.

In the current stage, the spring was selected based on the subjective judgment of an experienced physical therapist and based on the power output limitation of the current MRLink. Inspired by the works of Yamamoto *et al.* [13], we plan to introduce objective criteria in the selection of appropriate braking torque and spring coefficient to optimally implement SmartAFO for people with different levels of gait deficiencies. To this end, some methods will be needed to evaluate the ankle joint condition and to decide appropriate spring and braking parameters.

VI. Conclusion

In this paper, we presented the development of a linear elastic joint with MR fluid and a compression spring and a semiactive AFO based on the developed link. The experiments conducted with healthy people show that the developed AFO provided controllable braking at the initial contact phase and free plantarflexion at the push-off phase, and thus has the potential to mitigate toe-drag at the swing phase. This shows that a combination of passive components and smart material can form the basis for a robust and efficient wearable assistive technology. The viscosity modulation in an elastic link can translate into dynamic braking at the ankle joint, and in combination with a compression spring, can help achieve support functions without

requiring fully powered actuators. The power output of the developed MR device does not match with those of the wide range of AFOs used in practice. Further development in the core technology of MRLink will be needed to verify SmartAFO's benefit to the intended target population.

Acknowledgment

A part of the results is obtained from a project commissioned by the New Energy and Industrial Technology Development Organization.

References

[1] J. Perry, *Gait Analysis: Normal and Pathological Function*. Thorofare, NJ, USA: SLACK, 1992.
[2] M. Meinders, A. Gitter, and J. M. Czerniecki, "The role of ankle plantar flexor muscle work during walking," *Scand. J. Rehabil. Med.*, vol. 30, no. 1, pp. 39–46, 1998.
[3] A. T. Chika and A. L. Uchenna, "The prevalence and pattern of foot drop in a private orthopedic and trauma center, south east, Nigeria: A10 year retrospective analysis," *IOSR J. Dental Med. Sci.*, vol. 16, pp. 109–113, 2017.
[4] J. D. Stewart, "Foot drop: Where, why and what to do?," *Practical Neurol.*, vol. 8, no. 3, pp. 158–169, 2008.
[5] P. Stevens, "Prevalence of balance compromise in commonly treated patient populations: An introduction to the academy's state of the science conference on the effects of ankle-foot orthoses on balance," *J. Prosthetics Orthotics,* vol. 22, pp. P1–P3, 10 2010.
[6] J. Redford, *Orthotics Etcetera*, (ser. House Officer Series). Baltimore, MD, USA: Williams & Wilkins, 1986.
[7] G. Rose, *Orthotics: Principles and Practice*, (ser. Orthotics: Principles and Practice). Portsmouth, NH, USA: Heinemann Medical Books, 1986, no. v. 26.
[8] S. Yamamoto, M. Ebina, M. Iwasaki, S. Kubo, H. Kawai, and T. Hayashi, "Comparative study of characteristics of plastic AFOS," *J. Prosthetics Orthotics*, vol. 5, pp. 59/47–52/64, 1993.
[9] N. Ramstrand and S. Ramstrand, "Aaop state-of-the-science evidence report: The effect of ankle-foot orthoses on balance—A systematic review," *J. Prosthetics Orthotics*, vol. 22, pp. P4–P23, 2010.
[10] K. A. Shorter, J. Xia, E. T. Hsiao-Wecksler, W. K. Durfee, and G. F. Kogler, "Technologies for powered ankle-foot orthotic systems: Possibilities and challenges," *IEEE/ASME Trans. Mechatronics*, vol. 18, no. 1, pp. 337–347, Feb. 2013.
[11] S. Yamamoto, M. Ebina, S. Kubo, T. Hayashi, Y. Akita, and Y. Hayakawa, "Development of an ankle-foot orthosis with dorsiflexion assist, part 2: Structure and evaluation," *J. Prosthetics Orthotics*, vol. 11, no. 2, pp. 24–28, 1999.
[12] S. Yamamoto, M. Fuchi, and T. Yasui, "Change of rocker function in the gait of stroke patients using an ankle foot orthosis with an oil damper: Immediate changes and the short-term effects," *Prosthetics Orthotics Int.*, vol. 35, no. 4, pp. 350–359, 2011, pMID: 21948737.
[13] S. Yamamoto, M. Ebina, S. Miyazaki, H. Kawai, and T. Kubota, "Development of a new ankle-foot orthosis with dorsiflexion assist, Part 1: Desirable characteristics of ankle-foot orthoses for hemiplegic patients," *J. Prosthetics Orthotics*, vol. 9, no. 4, pp. 174–179, 1997.
[14] O. Yokoyama, H. Sashika, A. Hagiwara, S. Yamamoto, and T. Yasui, "Kinematic effects on gait of a newly designed ankle-foot orthosis with oil damper resistance: A case series of 2 patients with hemiplegia," *Archives Physical Med. Rehabil.*, vol. 86, no. 1, pp. 162–166, 2005.
[15] J. A. Blaya and H. Herr, "Adaptive control of a variable-impedance ankle-foot orthosis to assist drop-foot gait," *IEEE Trans. Neural Syst. Rehabil. Eng.*, vol. 12, no. 1, pp. 24–31, Mar. 2004.
[16] K. W. Hollander, R. Ilg, T. G. Sugar, and D. Herring, "An efficient robotic tendon for gait assistance," *J. Biomech. Eng.*, vol. 128, pp. 788–791, Mar. 2006.
[17] T. Kikuchi, S. Tanida, K. Otsuki, T. Yasuda, and J. Furusho, "Development of third-generation intelligently controllable ankle-foot orthosis with compact mr fluid brake," in *Proc. IEEE Int. Conf. Robot. Automat.*, May 2010, pp. 2209–2214.
[18] W. Svensson and U. Holmberg, "Ankle-foot-orthosis control in inclinations and stairs," in *Proc. IEEE Conf. Robot., Automat. Mechatronics*, Sep. 2008, pp. 301–306.
[19] T. Julius, W. Bettina, B. Malte, and K. Marc, "Designs and performance of microprocessor-controlled knee joints," *Biomedizinische Technik/Biomed. Eng.*, vol. 59, pp. 65–77, 2013.
[20] J. Furusho *et al.*, "Development of shear type compact MR brake for the intelligent ankle-foot orthosis and its control; research and development in nedo for practical application of human support robot," in *Proc. IEEE 10th Int. Conf. Rehabil. Robot.*, Jun. 2007, pp. 89–94.
[21] M. R. Jolly, J. W. Bender, and J. D. Carlson, "Properties and applications of commercial magnetorheological fluids," *J. Intell. Mater. Syst. Structures*, vol. 10, no. 1, pp. 5–13, 1999.
[22] S. Shimizu and K. Suzuki, "A force retention mechanism by MR spring for walking support," in *Proc. IEEE Int. Conf. Robot. Biomimetics*, Dec. 2009, pp. 1148–1153.
[23] D. Winter, *Biomechanics and Motor Control of Human Movement*. Hoboken, NJ, USA: Wiley, 2009.

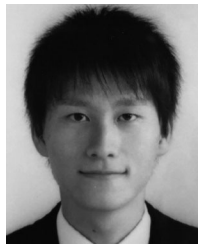

Takahiro Oba received the B.S. and M.E. degrees in engineering from the University of Tsukuba, Tsukuba, Japan, in 2012 and 2014.

He is currently working with NEC Corporation, Minato, Tokyo, Japan, and engaged in development of robotics related technologies. His research interests include assistive robotics and unmanned aerial vehicles.

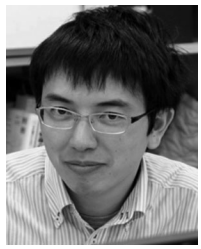

Hideki Kadone received the Ph.D. degree in information science and technology from the University of Tokyo, Tokyo, Japan, in 2008.

He is currently an Assistant Professor with Center for Innovative Medicine and Engineering, and Center for Cybernetics Research, Faculty of Medicine, University of Tsukuba, Tsukuba, Japan. His research interests include clinical motion measurement and analysis and development of wearable assistive devices to compensate for, support or improve motor function of patients after neurological or mechanical disorders.

Modar Hassan (M'16) received the B.S. degree in engineering from Tishreen University, Latakia, Syria, in 2009. He received M.E. and Ph.D. degrees in engineering in 2013 and 2016, and the M.S. degree in medical sciences from the University of Tsukuba, Tsukuba, Japan, in 2016.

From 2010 to 201, he was a Lecturer of mechatronics in Tishreen University. He is currently a Researcher at the Faculty of Engineering, Information and Systems, University of Tsukuba. His research interests include assistive robotics, orthotics, biomechanics, and motor control.

Kenji Suzuki (M'98) received the B.S. degree in physics, and the M.E. and Ph.D. degrees in pure and applied physics from Waseda University, Tokyo, Japan, in 1997, 2000 and 2003, respectively.

He is currently a Full Professor with the Center for Cybernics Research, and a Principal Investigator of Artificial Intelligence Laboratory, Faculty of Engineering, University of Tsukuba, Tsukuba, Japan. He was also a Visiting Researcher at the Laboratory of Physiology of Perception and Action, College de France in Paris, and the Laboratory of Musical Information, University of Genoa, Genoa, Italy. His research interests include augmented human technology, assistive and social robotics, humanoid robotics, biosignal processing, social playware, and affective computing.